# A TOCA/CDC-42/PAR/WAVE functional module required for retrograde endocytic recycling

Zhiyong Bai and Barth D. Grant[1]

Department of Molecular Biology and Biochemistry, Rutgers University, Piscataway, NJ 08854

Edited by Iva Greenwald, Columbia University, New York, NY, and approved February 13, 2015 (received for review September 26, 2014)

**Endosome-to-Golgi transport is required for the function of many key membrane proteins and lipids, including signaling receptors, small-molecule transporters, and adhesion proteins. The retromer complex is well-known for its role in cargo sorting and vesicle budding from early endosomes, in most cases leading to cargo fusion with the trans-Golgi network (TGN). Transport from recycling endosomes to the TGN has also been reported, but much less is understood about the molecules that mediate this transport step. Here we provide evidence that the F-BAR domain proteins TOCA-1 and TOCA-2 (Transducer of Cdc42 dependent actin assembly), the small GTPase CDC-42 (Cell division control protein 42), associated polarity proteins PAR-6 (Partitioning defective 6) and PKC-3/atypical protein kinase C, and the WAVE actin nucleation complex mediate the transport of MIG-14/Wls and TGN-38/TGN38 cargo proteins from the recycling endosome to the TGN in *Caenorhabditis elegans*. Our results indicate that CDC-42, the TOCA proteins, and the WAVE component WVE-1 are enriched on RME-1–positive recycling endosomes in the intestine, unlike retromer components that act on early endosomes. Furthermore, we find that retrograde cargo TGN-38 is trapped in early endosomes after depletion of SNX-3 (a retromer component) but is mainly trapped in recycling endosomes after depletion of CDC-42, indicating that the CDC-42–associated complex functions after retromer in a distinct organelle. Thus, we identify a group of interacting proteins that mediate retrograde recycling, and link these proteins to a poorly understood trafficking step, recycling endosome-to-Golgi transport. We also provide evidence for the physiological importance of this pathway in WNT signaling.**

retromer | endocytic recycling | endosome | *toca* | wave

Endocytosis mediates the internalization of cell-surface proteins and lipids in small vesicles that bud from the plasma membrane and deliver their cargo to endosomes (1). Once cargo proteins reach the endosomes, one important pathway they may follow is retrograde recycling, in which cargos are delivered from endosomes to the trans-Golgi network (TGN) (2). Many important membrane proteins, including signaling receptors and small molecular transporters, require retrograde recycling (2). Some well-studied examples include the cation-independent mannose 6-phosphate receptor, insulin-stimulated glucose transporter Glut4, and Wls/MIG-14, a protein that ferries Wnt ligands to the cell surface during their secretion (2, 3). Certain toxins and viruses co-opt such retrograde transport pathways during their toxic/infectious cycles. These include the bacterial toxins Shiga and cholera, plant exotoxins ricin and abrin, as well as adeno-associated virus type 5 (AAV5) and HIV-1 (2, 3).

Relatively few studies have focused on how such recycling pathways function in polarized epithelial cells, although polarized epithelia are a very abundant and important cell type in the human body. The intestine of the nematode *Caenorhabditis elegans* is a powerful model system for the study of endocytic recycling in the context of polarized epithelial cells, and can be studied within their normal context of the intact living animal (4, 5). The *C. elegans* intestine is a simple epithelial tube composed of 20 cells arranged mostly in pairs (6). Like mammalian intestinal epithelial cells, those of the *C. elegans* intestine display readily apparent apicobasal polarity, with basolateral and apical domains separated by apical junctions (6). The intestinal luminal (apical) membranes display a dense microvillar brush border with an overlying glycocalyx and subapical terminal web (6). The basolateral membrane faces the body cavity, exchanging molecules between the intestine and peripheral tissues.

We previously established several model transmembrane cargo markers for the analysis of basolateral endocytosis and recycling in the *C. elegans* intestine (5, 7–10). These include MIG-14-GFP, hTfR-GFP, and hTAC-GFP (5). MIG-14 (Wntless) and hTfR (human transferrin receptor) enter cells via clathrin-dependent endocytosis (5, 7, 11). hTAC (human IL-2 receptor α-chain) enters cells via clathrin-independent endocytosis (4, 5). hTfR and hTAC recycle to the plasma membrane via recycling endosomes, also known as the endocytic recycling compartment (4, 7). MIG-14 recycles to the TGN, but previous work had not tested whether MIG-14 transits the recycling endosome en route to the Golgi (12–14).

Many studies in cultured cell lines indicate that there are multiple routes to the Golgi from endosomes, including proposed routes from the recycling endosome, in addition to the more commonly discussed early endosome and late endosome routes (15–19). For instance, CHO cell pulse–chase analysis of fusion proteins bearing the transmembrane and intracellular domains of retrograde recycling proteins, TGN38 and Furin, showed that TGN38 trafficked from the early endosome to recycling endosome to the Golgi, whereas Furin recycling involved transit from the early endosome to the late endosome to the Golgi (20, 21). TGN38 and Shiga toxin have been shown to require distinct sets of SNARE proteins to complete transport to the Golgi, also indicating that different cargos recycle to the Golgi in different types of vesicles (22). In addition, TGN38 requires recycling endosome regulator Rab11 and its effector FIP1/RCP

## Significance

Endosomes are membrane-bound organelles that are required for the sorting of membrane-associated proteins and lipids. Once integral membrane proteins reach the endosomal system they can be sent to the lysosome for degradation, recycled to the plasma membrane, or recycled to the Golgi apparatus. Here we provide insight into the molecules that mediate a poorly understood route to the Golgi from recycling endosomes. The mediators of this transport step that we identified include the membrane-binding and -bending TOCA proteins, the small GTPase CDC-42, associated polarity proteins PAR-6 and PKC-3/atypical protein kinase C, and the WAVE actin nucleation complex. Many transmembrane proteins likely use this same transport mechanism.

Author contributions: Z.B. and B.D.G. designed research; Z.B. performed research; Z.B. and B.D.G. analyzed data; and Z.B. and B.D.G. wrote the paper.

The authors declare no conflict of interest.

This article is a PNAS Direct Submission.

[1]To whom correspondence should be addressed. Email: grant@biology.rutgers.edu.

This article contains supporting information online at www.pnas.org/lookup/suppl/doi:10.1073/pnas.1418651112/-/DCSupplemental.

for retrograde recycling, further indicating that the recycling endosome pathway is important in TGN38 retrieval to the Golgi (23). The recycling endosome regulator and dynamin superfamily-like ATPase EHD1/mRme-1 is also required for transport of several cargos from recycling endosomes to the Golgi (24–26). The cation-independent mannose 6-phosphate receptor has also been reported to require transport through the recycling endosome to reach the TGN (24, 25).

Previous whole-genome analysis of genes required for yolk protein endocytosis in the *C. elegans* oocyte, a process that requires yolk receptor recycling, identified the Rho-family GTPase CDC-42 and its associated proteins PAR-3 and PAR-6 (PDZ domain proteins), as well as the *C. elegans* homolog of atypical protein kinase C, PKC-3 (27). Together, these proteins are often referred to as the anterior PAR complex, because they function together to establish and maintain anterior–posterior polarity in the early *C. elegans* embryo (28). This work showed that CDC-42 is enriched on RME-1–positive recycling endosomes in nonpolarized *C. elegans* coelomocytes and cultured mammalian fibroblasts (27). These and other data implicated the CDC-42/PAR complex in recycling endosome function, but further mechanistic insight was lacking (27, 29, 30). Other work showed that CDC-42–associated Bar-domain proteins TOCA-1 and TOCA-2 function redundantly in yolk endocytosis, also probably functioning at a postendocytic transport step (31).

To better understand the function of the TOCA proteins, and potentially the anterior PAR complex, in membrane transport, we set out to analyze their function in the *C. elegans* intestine using the molecular tools that we had established in this tissue. Unlike the general recycling regulator RME-1, which affects all recycling cargo that we have tested in the *C. elegans* intestine, we found that *toca-1; toca-2* double mutants strongly affected MIG-14 but not hTAC or hTfR. Further analysis connected TOCA-1 and TOCA-2 to the CDC-42/PAR complex in this process, and further indicated that these proteins function with WVE-1, a core subunit of the actin nucleation complex WAVE. These results indicated a requirement for TOCA/CDC-42/PAR/WAVE in retrograde recycling, in addition to the well-known retromer complex, which contains a similar complement of molecules implicated in membrane binding, membrane bending, and actin nucleation. Finally, we established the *C. elegans* homolog of retrograde recycling cargo TGN38 (TGN-38) as a retrograde recycling cargo in the intestine. Experiments with GFP-tagged TGN-38 allowed us to compare the cargo transport blocks imposed by depletion of a subunit of the retromer complex (SNX-3) with the block imposed by depletion of CDC-42, as a representative of the TOCA/CDC-42/PAR/WAVE group (32). These experiments indicated a specific block at the early endosome after retromer depletion, whereas CDC-42 depletion blocked TGN-38 retrograde recycling most strongly at the recycling endosome. Taken together, these results demonstrate an important role for TOCA/CDC-42/PAR/WAVE acting at the recycling endosome after retromer function at the early endosome. We also provide evidence for the physiological importance of this pathway in WNT signaling, focusing on the polarity of the ALM mechanosensory neurons.

## Results

**Sorting of Recycling Cargo Proteins in *C. elegans* Intestinal Epithelia by TOCA Proteins.** To elucidate the step in endocytic transport requiring *C. elegans* TOCA proteins, we tested the effects of the *toca-1(tm2056); toca-2(ng11)* double mutant on the steady-state localization of recycling cargo proteins MIG-14-GFP, hTAC-GFP, and hTfR-GFP. We found that in *toca-1; toca-2* double mutants, but not *toca-1* or *toca-2* single mutants, MIG-14-GFP fluorescence is reduced by about two-thirds, an effect similar to known recycling mutants (Fig. 1 *A*, *B*, and *F* and *SI Appendix*, Fig. S1 *A*, *B*, *E*, *F*, *I*, *J*, and *M*). Anti-GFP Western blots confirmed reduction in MIG-14-GFP steady-state level in *toca* double mutants (Fig. 1*H*). hTfR-GFP and hTAC-GFP localization and fluorescence intensity were not reduced in *toca-1; toca-2* double mutants, suggesting a specific requirement for the TOCA proteins in retrograde recycling (*SI Appendix*, Fig. S1 *F* and *J*). Furthermore, none of the cargo markers appeared to increase in intensity on the plasma membrane in *toca-1; toca-2* double mutants, suggesting that the TOCA proteins are not important for cargo removal from the cell surface (Fig. 1*B* and *SI Appendix*, Fig. S1*B*).

To better understand which step in membrane traffic is defective in *toca* double mutant animals, leading to the loss of MIG-14 protein levels, we used RNAi-mediated depletion of APM-2 (DPY-23), the medium (mu) subunit of clathrin adapter AP-2. We found that blocking AP-2–dependent endocytosis in animals lacking TOCA-1 and TOCA-2 restored MIG-14 levels, trapping as much MIG-14-GFP at the plasma membrane as in wild-type animals depleted of APM-2 (Fig. 1*B′*). This result indicates that the defect in MIG-14 sorting in *toca* double mutants is postendocytic, likely resulting from defective sorting of MIG-14 within endosomes.

In retromer mutants, MIG-14 recycling to the TGN is blocked, and MIG-14 is missorted to the lysosome. This leads to increased MIG-14 degradation and reduced steady-state levels of the MIG-14 protein (12–14). Consistent with the idea that loss of the TOCA proteins also leads to missorting of MIG-14 into the degradative pathway, we found that more MIG-14-GFP colocalized with late endosome and lysosome marker tag RFP-RAB-7 in *toca* double mutant animals than in WT animals (*SI Appendix*, Fig. S2 *B–B′′*). Furthermore, we found that loss of MIG-14-GFP in *toca* double mutants depends upon lysosome function. In *cup-5*/mucolipin1 mutants, in which lysosome function is severely impaired, MIG-14-GFP protein level was restored, equivalent to the levels found in *cup-5* mutants with normal TOCA function (Fig. 1 *A′′*, *B′′*, and *G* and *SI Appendix*, Fig. S2) (12, 33). We conclude that the TOCA proteins are required for retrograde recycling of MIG-14, and that in the absence of TOCA proteins MIG-14 is missorted to the lysosome after endocytosis.

**TOCA Protein HR1 and SH3 Domains Are Required for Recycling Function.** To better understand the role of the TOCA proteins in MIG-14 recycling, we sought to test the importance of predicted protein interaction domains in TOCA-2 and to identify TOCA-binding proteins relevant to TOCA-mediated MIG-14 trafficking. TOCA proteins include three important domains. The N-terminal BAR domain forms a curved membrane-binding surface and is essential for TOCA-mediated membrane remodeling (34). The central HR1 domain links TOCA-family proteins to the Rho-family GTPase Cdc42 (31, 35). In fact, the mammalian TOCA proteins were originally identified as effectors of Cdc42 (35). The C-terminal SH3 domain is likely to link the TOCA proteins to additional effectors.

To test the importance of the HR1 and SH3 domains in TOCA-mediated MIG-14 recycling, we introduced point mutations into each of these domains of TOCA-2 and assayed their ability to rescue MIG-14 localization and abundance in *toca-1; toca-2* double mutants. For the TOCA-2 HR1 domain, we introduced mutation I413S, equivalent to a mammalian Toca1 mutation that disrupts binding to CDC-42 (35). For the TOCA-2 SH3 domain, we introduced mutation W585K, equivalent to a mammalian Toca1 mutation that disrupts SH3 binding to downstream effectors (35). Intestine-specific expression of wild-type TOCA-2-tagRFP, but not TOCA-2-tagRFP bearing HR1(I413S) or SH3(W585K) mutations, rescued MIG-14-GFP levels, indicating that both domains, and likely some of their binding partners, are required for the MIG-14 recycling process (Fig. 2 *A–F*). Although they lacked rescuing activity, TOCA-2-tagRFP bearing HR1(I413S) or SH3 (W585K) mutations appeared to be expressed and localized in a manner similar to wild-type TOCA-2-tagRFP (Fig. 2*I*).

**CDC-42 and Anterior PAR Complex Proteins Are Required for MIG-14 Recycling.** Because mammalian TOCA proteins are known to act as Cdc42 effectors in forming cell-surface protrusions, and our analysis indicated that the HR1 domain of TOCA-2 is required for TOCA-mediated recycling of MIG-14, we tested the physical and functional requirements for CDC-42 in MIG-14 recycling. In addition, because CDC-42/Cdc42 often functions with the anterior PAR complex [PAR-3, PAR-6, PKC-3/atypical (a)PKC] in mediating embryonic and cellular polarity, we also tested for PAR complex function in retrograde recycling (27, 36).

We found that the HR1 domains of *C. elegans* TOCA-1 and TOCA-2 bound to *C. elegans* CDC-42, and that the I413S mutation in the TOCA-2 HR1 domain abrogated this binding, as judged by GST-pull-down analysis (Fig. 2*G* and *SI Appendix*, Fig. S3). Furthermore, we found that after RNAi-mediated depletion of CDC-42 or PAR-6, MIG-14-GFP fluorescence as measured by confocal microscopy and MIG-14-GFP protein levels as measured by anti-GFP Western blot were strongly reduced (Fig. 1 *C*, *D*, *F*, and *H*). Consistent with defective endosomal sorting of MIG-14 in animals lacking CDC-42 and the PAR proteins, we found that more MIG-14-GFP colocalized with late endosome and lysosome marker tagRFP-RAB-7 in *cdc-42(RNAi)* and *pkc-3(RNAi)* animals than in wild-type animals (*SI Appendix*, Fig. S2 *C–C″* and *D–D″*). Finally, the loss of MIG-14-GFP after *cdc-42(RNAi)* or *par-6(RNAi)* could be blocked by disrupting AP-2–mediated endocytosis or lysosomal degradation, further indicating that the requirement for CDC-42 and PAR-6 is postendocytic and that CDC-42 and PAR-6 are required to prevent loss of MIG-14 to the lysosome, similar to the effect observed upon loss of TOCA-1 and TOCA-2 (Fig. 1 *C–D″* and *G*) (13, 14). Thus, we conclude that the CDC-42, PAR-6, and PKC-3 proteins are also required for MIG-14 recycling.

**The TOCA Proteins Link CDC-42 to the WAVE Complex.** The SH3 domains of mammalian TOCA proteins, and the GTP-bound conformation of Cdc42, have been shown to interact with actin regulator N-Wasp (4). Actin regulation on endosomes is thought to be important for cargo sorting processes (35). We did not find any change in MIG-14-GFP fluorescence intensity or localization in *C. elegans wsp-1*/Wasp mutants, suggesting that WSP-1 is not required for MIG-14 recycling (*SI Appendix*, Fig. S4 *A–C*).

Previous work showed binding of the *C. elegans* TOCA-2 SH3 domain, but not the *C. elegans* TOCA-1 SH3 domain, to *C. elegans*

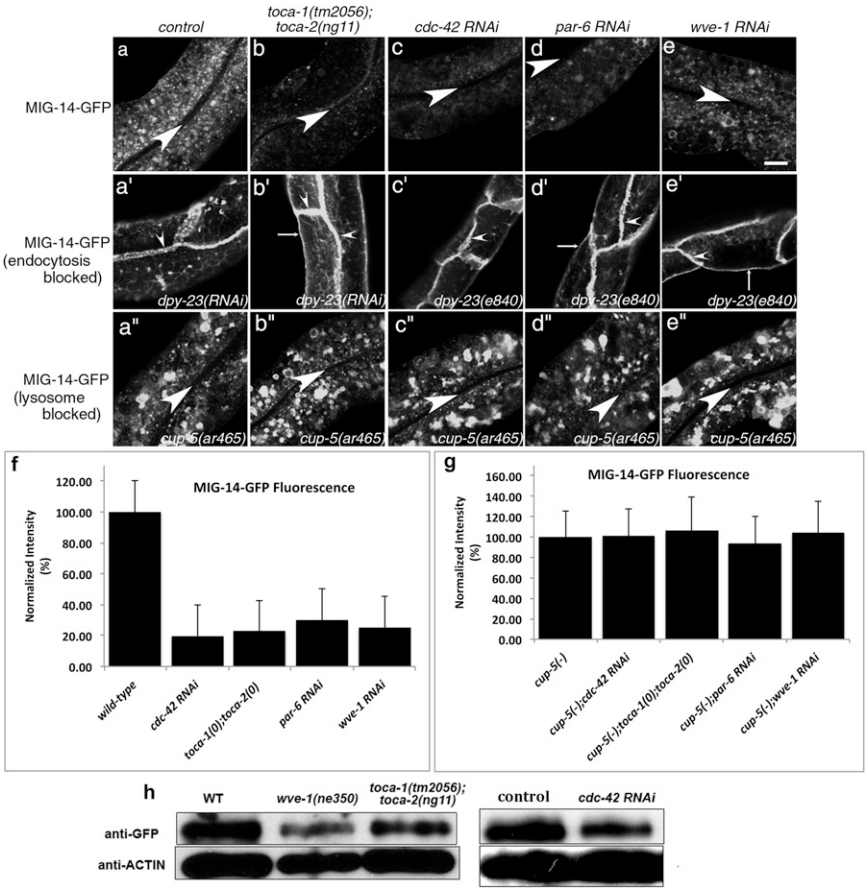


**Fig. 1.** MIG-14-GFP is missorted into the degradative pathway after endocytosis in the intestinal epithelia of *toca-1; toca-2* double mutants or after RNAi-mediated knockdown of *cdc-42*, *par-6*, or *wve-1*. (*A–E″*) Confocal images were acquired in intact living animals expressing GFP-tagged MIG-14/Wls specifically in the intestinal epithelial cells. (*A–E*) MIG-14-GFP fluorescence is shown in wild-type, *toca-1(tm2056); toca-2(ng11)* double mutant, *cdc-42(RNAi)*, *par-6(RNAi)*, or *wve-1(RNAi)* animals. (*A′–E′*) *dpy-23(e840)/apm-2* mutants, lacking the mu subunit of clathrin adapter AP-2, treated as in *A–E*. MIG-14-GFP, trapped at the basolateral plasma membrane due to an endocytosis block, was unaffected in a *toca-1(tm2056); toca-2(ng11)* double mutant, *cdc-42(RNAi)*, *par-6(RNAi)*, or *wve-1(RNAi)*. (*A″–E″*) *cup-5(ar465)* mutants, strongly impaired in lysosomal degradation, treated as in *A–E*, retained high levels of MIG-14-GFP in *toca-1 (tm2056); toca-2(ng11)* double mutant, *cdc-42(RNAi)*, *par-6(RNAi)*, or *wve-1(RNAi)*. Large arrowheads mark the intestinal lumen (enclosed by the apical membrane). Small arrowheads mark lateral membranes where cells meet side to side or end to end. Thin arrows indicate basal membranes. About one cell length of the intestine is shown in each panel. (Scale bar, 10 μm.) (*F* and *G*) Quantification of MIG-14-GFP integrated intensity for the indicated genotypes. Error bars in *F* and *G* represent SEM. (*H*) Anti-GFP and anti-actin Western blot analysis for animals of the indicated genotype and RNAi treatments. Control indicates empty vector RNAi.

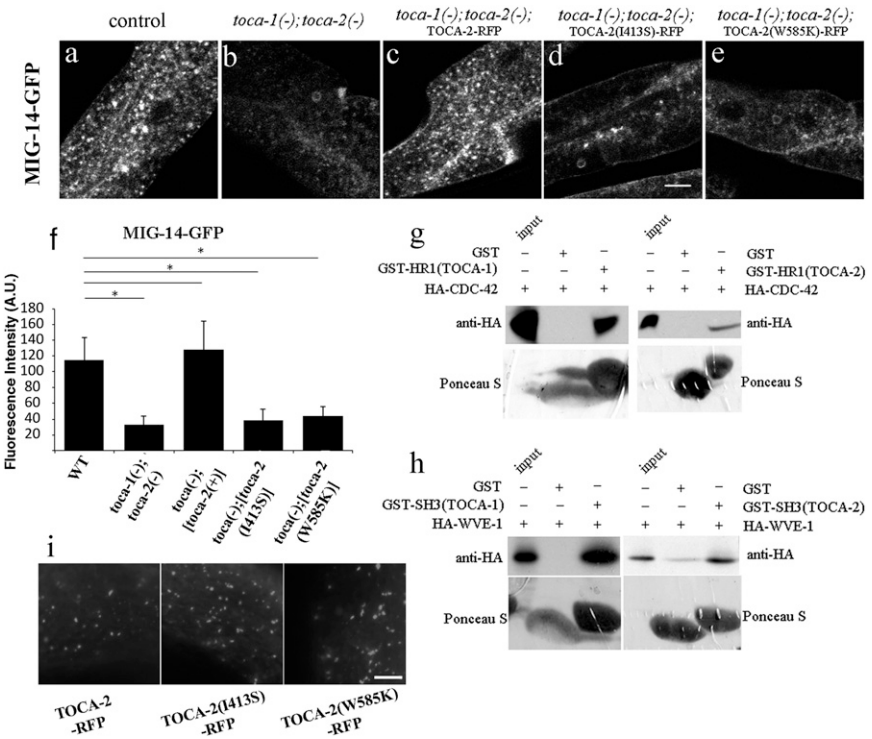


**Fig. 2.** TOCA-2 requires both SH3 and HR1 domains for its function in retrograde transport. (*A*–*E*) Confocal images of intestine-specific expression of GFP-tagged MIG-14/Wls acquired in intact living animals. Wild-type control, or *toca-1; toca-2* double mutants, are shown, with or without intestine-specific re-expression of GFP-tagged TOCA-2(+),TOCA-2(I413S) HR1 domain mutant, or TOCA-2(W585K) SH3 domain mutant. Note the loss of MIG-14-GFP in *toca-1 (tm2056); toca-2(ng11)* double mutants (*B*) and the restoration of MIG-14-GFP levels upon intestine-specific expression of wild-type TOCA-2 (*C*). MIG-14-GFP levels were not restored upon expression of TOCA-2(I413S) or TOCA-2(W585K) mutants (*D* and *E*). (Scale bar, 10 μm.) (*F*) Quantification of average integrated puncta intensity is shown. Error bars in *F* represent SEM. A.U., arbitrary units. $*P < 0.001$. (*G* and *H*) In vitro translated HA-tagged proteins, CDC-42(G12V) or WVE-1, were incubated with immobilized recombinant proteins, GST-only, GST-HR1 domain of TOCA-1 or TOCA-2 (*G*), or GST-SH3 domain of TOCA-1 or TOCA-2 (*H*). After washing, bound proteins were eluted by boiling and analyzed by Western blot with anti-HA antibody. Input lanes represent 20% of the original HA-tagged proteins. (*Lower*) Total GST-fusion bait proteins visualized by Ponceau S staining before antibody probing. (*I*) Micrographs of TOCA-2-tagRFP wild-type and mutant forms expressed in the *C. elegans* intestine. (Scale bar: 10 μm.)

ABI-1, a component of another actin regulatory complex called WAVE (31). It was also shown that mammalian TOCA-1 coimmunoprecipitates with mammalian ABI-1 in HeLa cells (31). Interestingly, recently published yeast two-hybrid and phage display analysis of the *C. elegans* SH3-ome identified another component of the WAVE complex, WVE-1/Wave1, as a high-probability TOCA-1–binding protein (37). Using a GST-pull-down assay, we found that the SH3 domains of TOCA-1 and TOCA-2 bound to WVE-1, whereas the W585K mutation in the TOCA-2 SH3 domain abrogated such binding (Fig. 2*H* and *SI Appendix*, Fig. S3).

Consistent with WVE-1 as an in vivo binding partner of the TOCA proteins relevant to MIG-14 recycling, we found that after RNAi-mediated depletion of WVE-1, MIG-14-GFP fluorescence as measured by confocal microscopy and MIG-14-GFP protein levels in *wve-1* mutant animals as measured by anti-GFP Western blot were strongly reduced (Fig. 1 *E*, *F*, and *H*). MIG-14-GFP fluorescence was also strongly reduced after RNAi of another WAVE complex component, GEX-3, suggesting a requirement for the entire WAVE core complex in MIG-14 retrograde recycling (*SI Appendix*, Fig. S4). Furthermore, we found increased MIG-14-GFP colocalization with late endosome and lysosome marker tagRFP-RAB-7 in *wve-1(RNAi)* animals (*SI Appendix*, Fig. S2 *E*–*E*″). In addition, the loss of MIG-14-GFP after *wve-1(RNAi)* could be blocked by disrupting AP-2–mediated endocytosis or lysosomal degradation, again indicating that the requirement for WVE-1 in MIG-14 trafficking is postendocytic (Fig. 1 *E*–*E*″, *G*, and *H*). Thus, we conclude that the WAVE complex is an important binding partner for TOCA-mediated MIG-14 recycling.

**TOCA/CDC-42/WAVE Proteins Are Enriched on Recycling Endosomes.** There are several possible steps in transport that might contribute to MIG-14 recycling to the Golgi. To help us understand where within the cell the TOCA proteins and their interactors function to direct MIG-14 recycling, we analyzed the subcellular localization of tagged fusion proteins expressed specifically in the intestinal epithelia from low-copy number transgenes. Tagged forms of TOCA-1 and TOCA-2 localized to intracellular puncta enriched in the basolateral cytoplasm and on the basolateral and apical plasma membrane (Fig. 3 *A* and *B* and *SI Appendix*, Fig. S5 *A* and *B*). TOCA-1 and TOCA-2 colocalized with one another, consistent with the genetic evidence that they are redundant (Fig. 3 *B*–*B*″). Among the compartment markers that we analyzed, TOCA-1-GFP colocalized with basolateral recycling endosome marker RME-1, indicating significant residence on recycling endosomes (Fig. 3 *A*–*A*″). Confirming this localization, we found that endosomes labeled with tagged TOCA-1 and TOCA-2 were grossly enlarged in *rme-1* mutants (*SI Appendix*, Fig. S5 *A*, *A*′, *B*, *B*′, *C*, and *D*). Our previous work established that only basolateral recycling endosomes, and not other endosome types, are enlarged in the intestine of *rme-1* mutants (7). In addition, TOCA-1-GFP failed to colocalize with early endosome marker RFP-RAB-5 or with Golgi marker RFP-RAB-6.2 (*SI Appendix*, Fig. S5 *E*–*E*″ and *G*–*G*″).

Consistent with a role for CDC-42 in regulation of TOCA-mediated trafficking, *cdc-42* RNAi resulted in an expansion of TOCA-1– and TOCA-2–labeled recycling endosomes similar to that produced by loss of RME-1 (*SI Appendix*, Fig. S5 *A*″, *B*″, *C*, and *D*). Furthermore, tagged CDC-42 and WVE-1 colocalized

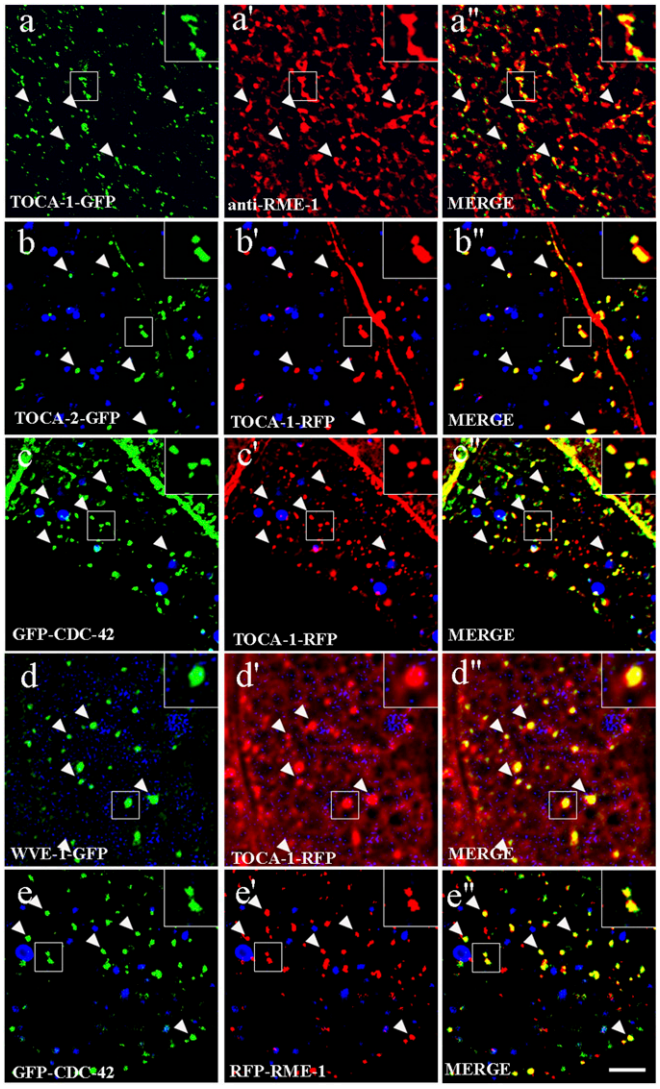


**Fig. 3.** TOCA proteins are enriched on recycling endosomes in the intestinal epithelia. Single planes from deconvolved wide-field image stacks are shown for *A–E″*. Confocal images are shown for *F–G″*. In *A–A″*, intestines from animals expressing TOCA-1-GFP were hand-dissected and stained with rabbit anti–RME-1 antibodies (81) and Alexa-568–conjugated anti-rabbit secondary antibodies. Note the colocalization of TOCA-1-GFP– and RME-1–labeled basolateral recycling endosomes. In *B–E″*, images were acquired in intact living animals expressing GFP- and/or RFP-tagged proteins in the intestinal epithelial cells. Note the colocalization to punctate endosomal structures (arrowheads). In each set of images, autofluorescent lysosome-like organelles can be seen in blue. GFP appears only in the green channel, and RFP appears only in the red channel. Signals observed in the green or red channels that do not overlap with signals in the blue channel are considered bona fide GFP or RFP signals, respectively. *Insets* are magnified 3×. (Scale bar, 10 μm.)

with TOCA-1 on recycling endosomes (Fig. 3 *C–D″*). The localization of CDC-42 to basolateral recycling endosomes in the intestinal epithelia is consistent with our previous work showing localization of CDC-42 to recycling endosomes in the *C. elegans* coelomocyte cells and mammalian CHO cells and work by others showing a requirement for mammalian Cdc42 in basolateral trafficking in Madin-Darby canine kidney cells (27, 38, 39). Taken together, these results suggest that the TOCA proteins, along with CDC-42/PARs and the WAVE complex, function together at the recycling endosome to promote return of endocytosed MIG-14 to the Golgi.

**Loss of Retromer Affects Early Endosome Morphology but Not That of TOCA-Positive Endosomes.** The retromer complex is most commonly reported to initiate retrograde cargo recycling from the early endosome (3). Consistent with this idea, we found that retromer marker SNX-3-RFP colocalized well with early endosome marker GFP-RAB-5 but not recycling endosome markers GFP-RME-1 or GFP-RAB-11 (*SI Appendix*, Fig. S6 *A–C″*). Furthermore, we found that in the *C. elegans* intestine, mutants lacking retromer components SNX-3, VPS-35, VPS-26, or VPS-29 showed gross accumulation of early endosomes positive for GFP-RAB-5 (Fig. 4 *A–E* and *K* and *SI Appendix*, Fig. S7). The same retromer mutants displayed a normal distribution of basolateral recycling endosome marker GFP-RME-1, further indicating a specific function for retromer in early endosome function (Fig. 4 *F–J* and *L*). Like GFP-RME-1, TOCA-1-GFP and TOCA-2-GFP were unperturbed by loss of retromer component VPS-35, further supporting the localization of the TOCA proteins to recycling endosomes and not early endosomes (*SI Appendix*, Fig. S8). Similarly, we did not find any effect of the *toca-1; toca-2* double mutant or RNAi knockdown of *cdc-42*, *par-6*, *pkc-3*, or *wve-1* on the localization of GFP-tagged retromer component VPS-35, supporting the idea that TOCA/CDC-42/PAR/WAVE functions independent of retromer (*SI Appendix*, Fig. S9). Taken together, our results suggest that a TOCA/CDC-42/PAR/WAVE module could function after retromer in retrograde recycling at the level of recycling endosome-to-Golgi transport.

**Retromer and TOCA/CDC-42/PAR/WAVE Are Required for TGN-38 Recycling at Distinct Steps.** As an additional assay to better determine whether TOCA/CDC-42/PAR/WAVE proteins are required for transport of cargo from recycling endosomes to the TGN, we focused a set of experiments on TGN-38, the *C. elegans* homolog of mammalian TGN38/TGN46 (40–42). We focused on TGN-38 because previous work in mammalian cells showed that when its recycling is blocked, TGN38 accumulates in the compartment from which its budding is impaired, and because TGN38 is transported from the plasma membrane to the TGN via recycling endosomes (endocytic recycling compartment) in the well-studied CHO cell model (20, 22–24, 43, 44).

Transmembrane proteins of the TGN38 family display highly conserved intracellular domains that contain known trafficking signals (*SI Appendix*, Fig. S10). *C. elegans* TGN-38 also displays extracellular sequence motifs rich in prolines and charged residues, as are found in TGN38 homologs in other species (*SI Appendix*, Fig. S10) (42). Expression of GFP-tagged *C. elegans* TGN-38 in the *C. elegans* intestine labeled intracellular puncta that we identified as typical Golgi ministacks positive for RFP-RAB-6.2 (Figs. 5 *A–A″* and 6*B*). Mutation of a conserved tyrosine (Y314) to alanine in the intracellular domain of *C. elegans* TGN-38 trapped the protein at the basolateral cell surface, similar to results obtained in mammalian cells expressing TGN38 with the equivalent tyrosine mutation (Fig. 6 *A* and *H*) (45, 46). These results indicated that TGN-38-GFP can serve as cargo marker for retrograde transport from the basolateral plasma membrane to the TGN in the *C. elegans* intestine.

Consistent with retrieval of *C. elegans* TGN-38 from endosomes to the TGN after endocytosis, as has been shown in mammalian cells, we found that TGN-38-GFP accumulated in numerous large intracellular structures outside of the Golgi after *snx-3* RNAi and in similar aberrant structures in retromer mutants *vps-35*, *snx-3*, and *vps-29* (Figs. 5 *B–B″* and 6 *B–E*). Loss of these retromer components did not affect TGN-38(Y314A)-GFP, which is trapped at the basolateral surface, indicating that the effect of retromer on TGN-38 trafficking is postendocytic and does not reflect a defect in TGN-38 secretion (Fig. 6 *H–K*). Furthermore, upon RNAi-mediated depletion of retromer component *snx-3*, TGN-38-GFP accumulated in tagRFP-RAB-5–labeled early endosomes and not tagRFP-RME-1–labeled recycling

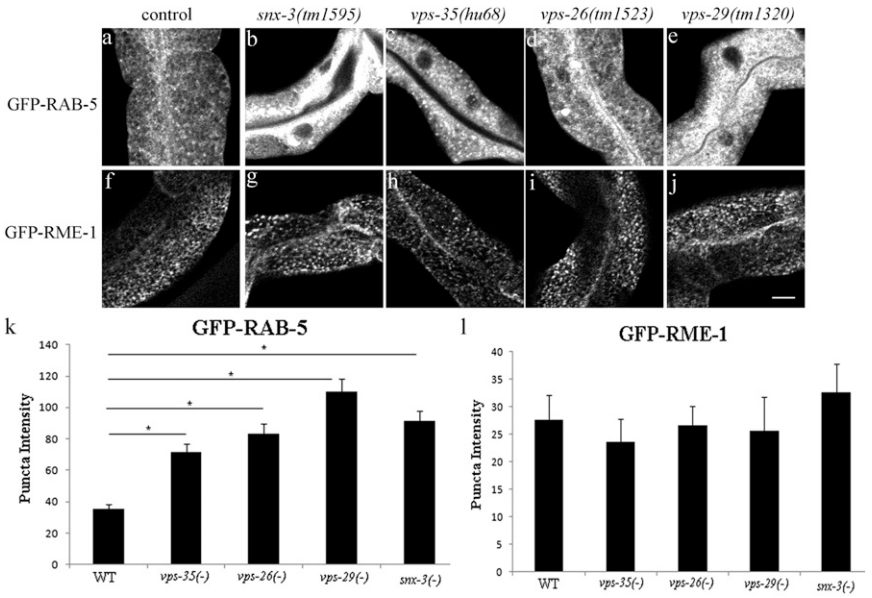


**Fig. 4.** Retromer mutants strongly affect early endosome morphology but not the morphology of RME-1– or TOCA protein-labeled recycling endosomes. Confocal images of *C. elegans* intestinal cells expressing early endosome marker GFP-RAB-5 (*A*–*C*) and basolateral recycling endosome marker GFP-RME-1 (*F*–*J*) in WT, *vps-35*, *vps-26*, *vps-29*, or *snx-3* mutant animals. (Scale bar, 10 μm.) (*K* and *L*) Quantification of endosome marker intensity in the noted genotypes. Error bars represent SEM. *$P < 0.001$. Note that early endosome marker GFP-RAB-5, rather than recycling endosome marker GFP-RME-1, is abnormal in retromer mutants.

endosomes (Fig. 7 *A*–*B″*, *D*–*E″*, and *G*). These results indicate a requirement for retromer in TGN-38 recycling at the level of the early endosome.

We also found accumulation of TGN-38-GFP in numerous large intracellular structures in *rme-1* mutants, *toca-1; toca-2* double mutants, and animals depleted of *cdc-42*, *pkc-3*, *par-6*, or *wve-1* by RNAi (Fig. 6 *F*, *G*, and *O*–*R*, and *SI Appendix*, Fig. S10*C*). Furthermore, loss of these recycling endosome-associated proteins did not affect TGN-38(Y314A)-GFP, indicating that the effect of these mutants or RNAi treatments on TGN-38 trafficking is postendocytic and does not reflect a delay in TGN-38 secretion (Fig. 6 *L*, *M*, and *T*–*W*). Importantly, we found that RNAi-mediated depletion of *cdc-42*, serving as a representative of the TOCA/CDC-42/PAR/WAVE group, resulted in high levels of TGN-38-GFP accumulation in tagRFP-RME-1–labeled recycling endosomes and, to a lesser extent, accumulation in tagRFP-RAB-5–labeled early endosomes, and reduced localization of TGN-38-GFP with the TGN, as marked by tagRFP-RAB-6.2 (Figs. 5 *C*–*C″* and 7 *C*–*C″*, *F*–*F″*, and *G*). This retrograde transport defect was quite distinct from that caused by loss of retromer. Taken together, these results indicate a requirement for TOCA/CDC-42/PAR/WAVE and RME-1 in a distinct retrograde recycling step, from recycling endosomes to the TGN.

**Neuronal Polarity Defects Are Observed upon Loss of TOCA/CDC-42/PARs/WAVE.** To test the physiological significance of recycling endosome-to-Golgi transport via the TOCA/CDC-42/PAR/WAVE pathway, we assayed its effect on WNT signaling, which depends upon the proper recycling of MIG-14/Wls in WNT ligand-secreting cells (12–14). WNT signaling strongly influences diverse polarized cell processes including the polarized growth of the *C. elegans* mechanosensory neuron ALM (47). In retromer mutants, where the retrograde recycling of MIG-14/Wntless is defective, WNT ligands such as EGL-20 are poorly secreted and WNT-mediated cell polarity is impaired (13, 14). Because we found reduced levels of MIG-14 in animals lacking the TOCA proteins, CDC-42/PARs, or WAVE complex components, we sought to determine whether WNT signaling is impaired upon loss or knockdown of these proteins. A defect in ALM neuronal polarity under such conditions would support a physiological role for these proteins in MIG-14 retrograde transport.

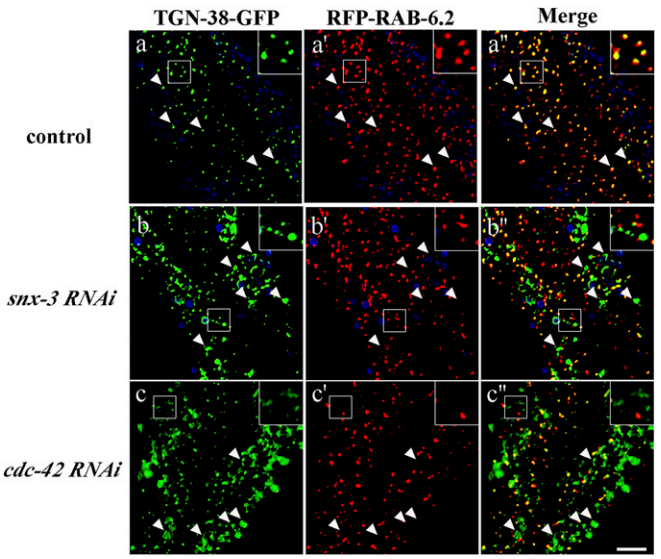


**Fig. 5.** Loss of CDC-42 or SNX-3 traps TGN-38-GFP outside the Golgi. Images were acquired in intact living animals coexpressing GFP-tagged TGN-38 and RFP-tagged Golgi marker RAB-6.2 in RNAi empty vector control (*A*–*A″*) or after *snx-3* (*B*–*B″*) or *cdc-42* RNAi (*C*–*C″*). Note that in control animals, most TGN-38 colocalizes with Golgi marker RAB-6.2, whereas large accumulations of TGN-38-GFP appear outside of the RAB-6.2–labeled Golgi after *snx-3* or *cdc-42* RNAi. In each set of images, autofluorescent lysosome-like organelles can be seen in blue. GFP appears only in the green channel, and RFP appears only in the red channel. Signals observed in the green or red channels that do not overlap with signals in the blue channel are considered bona fide GFP or RFP signals, respectively. *Insets* are magnified 3×. Arrowheads indicate the position of TGN-38 positive structures. (Scale bar, 10 μm.)

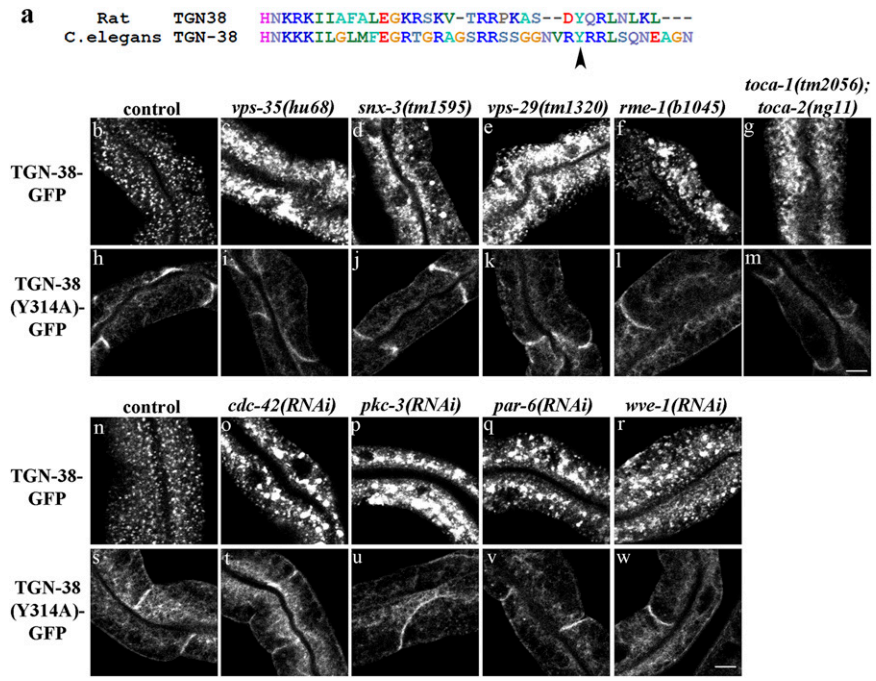


**Fig. 6.** *C. elegans* TGN-38-GFP localization depends upon retromer, RME-1, CDC-42, TOCA-1/TOCA-2, PAR-6, PKC-3, and WVE-1/WAVE. (*A*) An alignment of intracellular domains of rat TGN38 and *C. elegans* TGN-38 is shown. Conserved endocytosis signal Y314 is marked with an arrowhead. (*B–G* and *N–R*) Confocal images of *C. elegans* intestinal cells expressing GFP-tagged TGN-38 in the marked genotypes. (*H–M* and *S–W*) Endocytosis-defective Y314A mutant version of TGN-38-GFP in the indicated genetic backgrounds. Note the increase in TGN-38-GFP intensity upon loss of retromer, RME-1, CDC-42, TOCA-1/TOCA-2, PAR-6, PKC-3, or WVE-1. The endocytosis-defective Y314A version of TGN-38-GFP was unaffected, indicating the requirement for these trafficking factors in post-endocytic trafficking of TGN-38. (Scale bars, 10 μm.)

We analyzed the polarity of GFP-labeled ALM neurons in *toca-1(tm2056); toca-2(ng11)* double mutants and in animals depleted of *cdc-42*, *par-6*, or *wve-1* by RNAi. In each of these mutant or RNAi backgrounds, we observed a small but reproducible ALM polarity defect (5–15%) that was not present in control animals (*SI Appendix*, Fig. S11 and Table S1). Furthermore, we sought to determine whether *toca-1(tm2056); toca-2(ng11)* double mutant, or RNAi-mediated depletion of *cdc-42* or *par-6* by RNAi, effects on ALM polarity are enhanced by retromer mutant *vps-29(tm1320)*. Previous work showed that the Wnt phenotype of *vps-29(tm1320)* is much weaker than that of *vps-26* or *vps-35* mutants but shows enhanced phenotypes when combined with mutations in known Wnt-pathway components or retrograde recycling regulators (13, 48–50). Consistent with published work, we observed only normal ALM polarity in *vps-29(tm1320)* single mutants (47). However, the penetrance of ALM polarity defects in *toca-1; toca-2* double mutants increased by fourfold when combined with *vps-29(tm1320)* (*SI Appendix*, Table S1). We also observed a significant increase in the penetrance of ALM polarity defects after *cdc-42(RNAi)*, *par-6(RNAi)*, or *wve-1(RNAi)* comparing control and *vps-29(tm1320)* mutants (*SI Appendix*, Table S1). Finally, we tested whether disruption of CDC-42 function specifically in WNT-secreting cells impairs WNT signaling. To do this, we drove expression of GTPase-defective CDC-42(G12V) using the *egl-20* promoter, which directs expression to a group of WNT-secreting epidermal and muscle cells in the tail. Another *C. elegans* WNT ligand, CWN-1, which is broadly expressed in body-wall muscle cells, is redundant with EGL-20 in regulating ALM polarity (51). Consistent with the idea that CDC-42 is important for EGL-20 secretion, we found that *egl-20* promoter-driven expression of CDC-42(G12V), in a *cwn-1(ok546)* mutant background, produced significant ALM polarity defects, whereas *cwn-1* mutants alone showed no defects in ALM polarity (*SI Appendix*, Table S2). Taken together, these results strongly support a physiologically important role for the TOCA proteins, CDC-42, PAR-6, and WVE-1 in MIG-14–mediated WNT signaling.

## Discussion

Over the past 20 y, a number of regulators of retrograde recycling have been identified, the most prominent of which include the retromer and WASH complexes (52). These complexes are thought to work together on early and late endosomes to promote the budding of retrograde recycling vesicles. Our data presented here indicate an important role for a distinct group of proteins in retrograde recycling. The TOCA proteins, with CDC-42, PAR-6, PKC-3, and WVE-1/WAVE, together present a similar complement of functional molecular modules as retromer/WASH, with the potential to bind and bend membranes, nucleate actin, and perhaps recruit cargo. Our data, presented in this report, clearly indicate that the TOCA/CDC-42/PAR/WAVE group of interacting proteins is enriched on recycling endosomes, and all function in retrograde transport from the recycling endosome to the Golgi. Analysis of neuronal polarity indicates that this function is important for normal cellular signaling processes during development.

Although controversial, there is growing evidence that the recycling endosome (endocytic recycling compartment) plays an important role in the retrograde transport of some cargos to the TGN (15–19, 53). For instance, in mammalian cell pulse–chase experiments, TGN38 and Shiga toxin have been shown to be retrograde cargos that traverse the recycling endosome en route to the TGN (20, 21, 25). Canonical recycling endosome regulators Rab11, FIP1/RCP, and mRme-1/EHD1 have been shown to be important regulators of recycling endosome-to-TGN transport of retrograde cargo (23, 25, 54). However, the overall molecular mechanisms mediating this transport step have remained elusive.

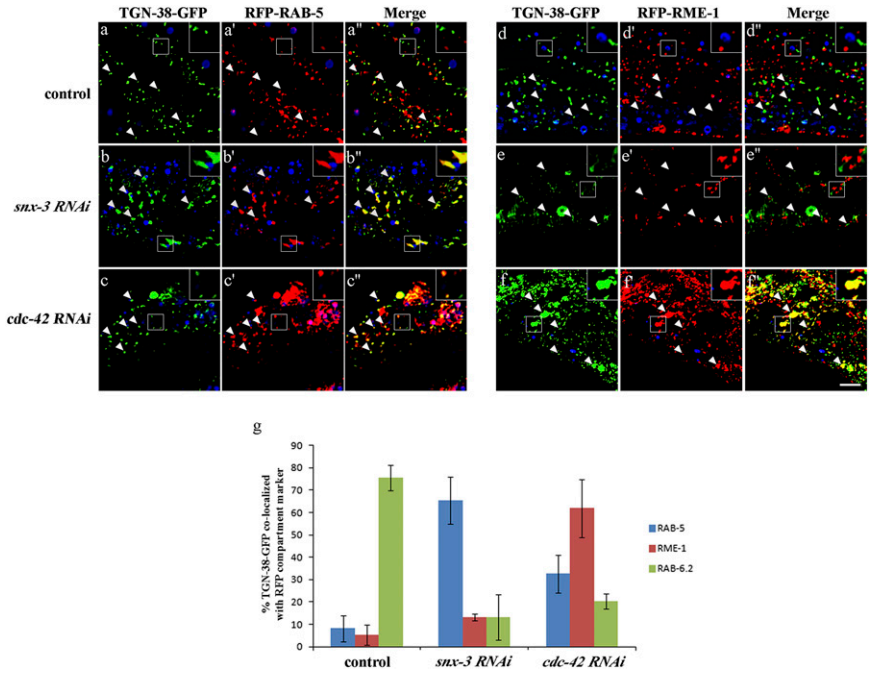


**Fig. 7.** SNX-3 and CDC-42 regulate TGN-38 retrograde transport at different transport steps. Images were acquired in intact living animals coexpressing GFP-tagged TGN-38 and RFP-tagged early (RAB-5) or recycling (RME-1) endosome markers. (*A–A″* and *D–D″*) In wild-type animals, very little TGN-38-GFP colocalizes with early endosome marker GFP-RAB-5 or recycling endosome marker GFP-RME-1. (*B–B″* and *E–E″*) In *snx-3* RNAi animals, TGN-38-GFP colocalization with early endosome marker RAB-5 increased strongly. (*C–C″* and *F–F″*) In *cdc-42* RNAi animals, TGN-38-GFP colocalization with recycling endosome marker RME-1 increased strongly. In each set of images, autofluorescent lysosome-like organelles can be seen in blue. GFP appears only in the green channel, and RFP appears only in the red channel. Signals observed in the green or red channels that do not overlap with signals in the blue channel are considered bona fide GFP or RFP signals, respectively. Arrowheads indicate the position of TGN-38 positive structures. Insets are magnified 3×. (Scale bar, 10 μm.) (*G*) Quantification of colocalization between TGN-38-GFP and RFP endosome markers. Error bars represent SEM.

Because the TOCAs/CDC-42/PAR/WAVE proteins bear functional domains that appear at least partly redundant with those in retromer/WASH but both sets of protein complexes are required for the recycling of MIG-14/Wls and TGN-38, we favor a model where retromer/WASH and TOCAs/CDC-42/PAR/WAVE protein complexes function sequentially, rather than at the same step. The apparent lack of colocalization of retromer with TOCAs/CDC-42 supports the idea of sequential function on different endosomal organelles along the recycling pathway. Our localization data in the worm intestinal epithelia indicate enrichment of retromer on early endosomes, as is commonly reported in other organisms and cell types, whereas we found that the TOCAs/CDC-42/PAR/WAVE proteins are enriched with RME-1 on basolateral recycling endosomes in these cells. In addition, our analysis of TGN-38 recycling fits a model in which TOCAs/CDC-42/PAR/WAVE function at the recycling endosome. We found that the loss of retromer component SNX-3 led to TGN-38 accumulation in early endosomes, whereas loss of CDC-42 caused the greatest accumulation of TGN-38 in the basolateral recycling endosome. Thus, we favor a model where some retrograde recycling vesicles formed at the early endosome, via retromer, traffic directly to the Golgi, whereas other retromer-derived vesicles fuse with the recycling endosome and require additional cargo sorting and cargo budding to reach the TGN. Although we do not know of an interaction between TOCAs/CDC-42/PAR/WAVE and retromer, it remains possible that such interactions exist, as many interactions are thought to occur between protein complexes acting in sequential transport steps, acting to hand off cargo and coordinate sequential activities (55). It also remains to be determined whether the TOCAs/CDC-42/PAR/WAVE proteins function in retrograde recycling in all cells, or whether their function in this pathway may be specific to certain cell types, such as polarized epithelia, which have more complex sorting needs because of their unique functions and architecture (56).

Work in *Drosophila* indicates that a role for Cdc42 and PAR proteins in retrograde recycling may be evolutionarily conserved. In the developing *Drosophila melanogaster* neuroectodermal epithelium, Cdc42, Par6, and aPKC are required to maintain the stability of dynamic apical junctions, because they regulate the subcellular localization of the transmembrane polarity regulator Crumbs (30). Upon loss of Cdc42, Par6, or aPKC, Crumbs is missorted to endosomes bearing degradative pathway markers, and Crumbs steady-state levels are strongly reduced (30). Analysis of Crumbs trafficking by other groups showed that Crumbs requires retromer-mediated retrograde recycling to maintain its plasma membrane localization and to avoid degradation in lysosomes (57, 58). Although not proposed in the published work, these studies suggest that Cdc42, Par6, and aPKC are likely to be required for retrograde recycling in *Drosophila*, as we have proposed here in *C. elegans*. In addition, work in fission yeast and polarized mammalian cells also suggests a requirement for Cdc42 in endocytic recycling (38, 59, 60). Thus, CDC-42 and associated protein function in retrograde recycling likely have an ancient origin and a widely conserved function.

Some proteins of the TOCA/CDC-42/PAR/WAVE group may also function separately at other transport steps. Although we did not find any colocalization between TOCA-1/TOCA-2 and early endosomes, previous work in cultured mammalian cells has indicated that CIP4, a TOCA-family protein, can be recruited to early endosomes by the activity of the EGF receptor, and somehow promotes the degradation of the EGF receptor in this context (61). One possible mechanism to explain this observation would be that recruiting TOCAs to the early endosome inhibits recycling via the recycling endosome, leading to EGF-receptor degradation. Previous work has also suggested a requirement for

the activity of the Arp2/3 and WAVE complexes in basolateral uptake of the human transferrin receptor expressed in the *C. elegans* intestine (62). We did not observe plasma membrane accumulation of MIG-14 or TGN-38 upon depletion of WVE-1, although depletion of ARP-2 did trap MIG-14-GFP on the basolateral plasma membrane, similar to the effect of depleting Dynamin (*SI Appendix*, Fig. S12). These results indicate that WAVE is not required for all clathrin/AP-2–dependent cargo uptake from the basolateral intestine, but Arp2/3 may be generally required for clathrin-dependent endocytosis in this context.

The retromer complex includes components that bind to transmembrane cargo and components proposed to bend membranes and/or sense membrane curvature, whereas the WASH complex nucleates the formation of branched actin networks (52). The TOCA, CDC-42, PAR, and WAVE proteins, along with RME-1/EHD, may also function in an endosomal vesicle-budding process important for retrograde recycling. The TOCA F-BAR domains are capable of membrane bending and potentially capable of membrane curvature sensing, activities that are essential for vesicle budding (63–65). We found that the SH3 domain of the TOCA proteins can interact with the VCA-containing WVE-1 protein, a component of the WAVE complex. VCA domains bind and activate ARP2/3 to promote local branched actin polymerization (66). The WAVE complex is well-known for its roles in promoting actin-based plasma membrane protrusion and cell motility (66, 67). Our data indicate that WAVE also functions in endocytic recycling. In mammals, the ARP2/3-stimulating VCA domain of WAVE2 is thought to be autoinhibited within the WAVE complex, and interaction with a variety of upstream regulators relieves this inhibition (66, 67). Thus, interaction of the TOCA SH3 domains with the WVE-1 proline-rich domain could promote recruitment and activation of WAVE on endosomal membranes. Importantly, the WAVE complex was also recently shown to interact directly with the intracellular domains of a large number of transmembrane proteins, and thus WAVE could also act to recruit cargo proteins during vesicle budding (68). Such an interaction could also help to activate WAVE, coordinating local ARP2/3-dependent actin polymerization with cargo loading.

Local actin polymerization is associated with many membrane-budding processes (69–72). Such actin polymerization has been proposed to increase local membrane tension and/or strain at lipid domain boundary regions (line tension), processes thought to promote membrane fission (69–71). Alternatively, actin polymerization has also been proposed to stabilize membrane buds or tubules, allowing time for cargo loading (73). CDC-42 is a known regulator of TOCA proteins in other processes, and could function, along with the CDC-42–interacting PAR proteins, to control the activity of the TOCA proteins during vesicle budding. Our data also suggest that the dynamin superfamily-related RME-1 ATPase functions in the TOCA retrograde recycling pathway. Further work will focus on understanding the functional relationships between these proteins in regulating endosomal function.

## Materials and Methods

**RNAi Analysis.** RNAi was performed by the feeding method (74). Feeding constructs including *apm-2/dpy-23*, *cdc-42*, *par-6*, *pkc-3*, *snx-3*, and *dyn-1* were from the Ahringer library (75). *wve-1* and *arp-2* feeding constructs were a generous gift from Martha Soto (Robert Wood Johnson Medical School, Piscataway, NJ) (62). For most experiments, synchronized first larval (L1) stage worms were used for RNAi assays. Phenotypes were scored in young adults. For colocalization studies, L4-stage worms applied to RNAi feeding plates and phenotypes were scored in L3- or L4-stage Filial 1 (F1) animals in the next generation.

**Microscopy and Image Analysis.** Transgenic worm lines were made using the microparticle bombardment method into *unc-119(ed3)* mutant animals to establish low-copy integrated transgenic lines (76, 77). Live worms were mounted on 2% (mass/vol) agarose pads with 10 mM levamisol as described previously (78). Multiwavelength fluorescence images were obtained using an Axiovert 200M (Carl Zeiss MicroImaging) microscope equipped with a digital CCD camera (QImaging; Rolera EM-$C^2$), captured using MetaMorph 7.7 software (Universal Imaging) and then deconvolved using AutoDeblur X3 software (AutoQuant Imaging). Images taken in the DAPI channel were used to identify broad-spectrum intestinal autofluorescence caused by lipofuscin-positive lysosome-related organelles (79, 80). Most GFP/RFP colocalization analysis was performed on L3 or L4 larvae. Some colocalization analysis was done using a spinning disk confocal microscope equipped with a confocal imager (CARV II; BD Biosciences) and a 63× oil objective lens. To obtain images of GFP fluorescence without interference from autofluorescence, we used the spectral fingerprinting function of a Zeiss LSM510 Meta confocal microscope system focusing on the 510-nm emission wavelength (Carl Zeiss MicroImaging). Quantification of images was performed with MetaMorph software (Universal Imaging) or ImageJ (National Institutes of Health). ALM neuron polarity was scored as in ref. 12. SDs and *t* test analysis were performed in Microsoft Excel.

**ACKNOWLEDGMENTS.** We thank Martha Soto for *wve-1* and *arp-2* RNAi clones. We thank Peter Schweinsberg for expert technical assistance. We thank Chris Rongo and Hilary Wilkinson for helpful comments on the manuscript. This work was supported by NIH Grants GM067237 and GM103995 (to B.D.G.) and an Anne B. and James B. Leathem Fellowship (to Z.B.).

1. McMahon HT, Boucrot E (2011) Molecular mechanism and physiological functions of clathrin-mediated endocytosis. *Nat Rev Mol Cell Biol* 12(8):517–533.
2. Burd CG (2011) Physiology and pathology of endosome-to-Golgi retrograde sorting. *Traffic* 12(8):948–955.
3. Seaman MN (2012) The retromer complex – endosomal protein recycling and beyond. *J Cell Sci* 125(Pt 20):4693–4702.
4. Grant BD, Donaldson JG (2009) Pathways and mechanisms of endocytic recycling. *Nat Rev Mol Cell Biol* 10(9):597–608.
5. Sato K, Norris A, Sato M, Grant BD (2014) *C. elegans* as a model for membrane traffic. *WormBook* 1–47.
6. McGhee JD (2007) The *C. elegans* intestine. *WormBook* 1–36.
7. Chen CC, et al. (2006) RAB-10 is required for endocytic recycling in the *Caenorhabditis elegans* intestine. *Mol Biol Cell* 17(3):1286–1297.
8. Sun L, et al. (2012) CED-10/Rac1 regulates endocytic recycling through the RAB-5 GAP TBC-2. *PLoS Genet* 8(7):e1002785.
9. Shi A, et al. (2010) EHBP-1 functions with RAB-10 during endocytic recycling in *Caenorhabditis elegans*. *Mol Biol Cell* 21(16):2930–2943.
10. Shi A, et al. (2007) A novel requirement for *C. elegans* Alix/ALX-1 in RME-1-mediated membrane transport. *Curr Biol* 17(22):1913–1924.
11. Gu M, et al. (2013) AP2 hemicomplexes contribute independently to synaptic vesicle endocytosis. *eLife* 2:e00190.
12. Shi A, et al. (2009) Regulation of endosomal clathrin and retromer-mediated endosome to Golgi retrograde transport by the J-domain protein RME-8. *EMBO J* 28(21):3290–3302.
13. Yang PT, et al. (2008) Wnt signaling requires retromer-dependent recycling of MIG-14/Wntless in Wnt-producing cells. *Dev Cell* 14(1):140–147.
14. Pan CL, et al. (2008) *C. elegans* AP-2 and retromer control Wnt signaling by regulating MIG-14/Wntless. *Dev Cell* 14(1):132–139.
15. Taguchi T (2013) Emerging roles of recycling endosomes. *J Biochem* 153(6):505–510.
16. Johannes L, Wunder C (2011) Retrograde transport: Two (or more) roads diverged in an endosomal tree? *Traffic* 12(8):956–962.
17. Pfeffer SR (2009) Multiple routes of protein transport from endosomes to the trans Golgi network. *FEBS Lett* 583(23):3811–3816.
18. Johannes L, Popoff V (2008) Tracing the retrograde route in protein trafficking. *Cell* 135(7):1175–1187.
19. Bonifacino JS, Rojas R (2006) Retrograde transport from endosomes to the trans-Golgi network. *Nat Rev Mol Cell Biol* 7(8):568–579.
20. Mallet WG, Maxfield FR (1999) Chimeric forms of furin and TGN38 are transported with the plasma membrane in the trans-Golgi network via distinct endosomal pathways. *J Cell Biol* 146(2):345–359.
21. Lee S, et al. (2012) Impaired retrograde membrane traffic through endosomes in a mutant CHO cell defective in phosphatidylserine synthesis. *Genes Cells* 17(8):728–736.
22. Lieu ZZ, Gleeson PA (2010) Identification of different itineraries and retromer components for endosome-to-Golgi transport of TGN38 and Shiga toxin. *Eur J Cell Biol* 89(5):379–393.
23. Jing J, et al. (2010) FIP1/RCP binding to Golgin-97 regulates retrograde transport from recycling endosomes to the trans-Golgi network. *Mol Biol Cell* 21(17):3041–3053.
24. Lin SX, Grant B, Hirsh D, Maxfield FR (2001) Rme-1 regulates the distribution and function of the endocytic recycling compartment in mammalian cells. *Nat Cell Biol* 3(6):567–572.

25. McKenzie JE, et al. (2012) Retromer guides STxB and CD8-M6PR from early to recycling endosomes, EHD1 guides STxB from recycling endosome to Golgi. *Traffic* 13(8):1140–1159.
26. Gleason RJ, Akintobi AM, Grant BD, Padgett RW (2014) BMP signaling requires retromer-dependent recycling of the type I receptor. *Proc Natl Acad Sci USA* 111(7):2578–2583.
27. Balklava Z, Pant S, Fares H, Grant BD (2007) Genome-wide analysis identifies a general requirement for polarity proteins in endocytic traffic. *Nat Cell Biol* 9(9):1066–1073.
28. Goldstein B, Macara IG (2007) The PAR proteins: Fundamental players in animal cell polarization. *Dev Cell* 13(5):609–622.
29. Harris KP, Tepass U (2010) Cdc42 and vesicle trafficking in polarized cells. *Traffic* 11(10):1272–1279.
30. Harris KP, Tepass U (2008) Cdc42 and Par proteins stabilize dynamic adherens junctions in the *Drosophila* neuroectoderm through regulation of apical endocytosis. *J Cell Biol* 183(6):1129–1143.
31. Giuliani C, et al. (2009) Requirements for F-BAR proteins TOCA-1 and TOCA-2 in actin dynamics and membrane trafficking during *Caenorhabditis elegans* oocyte growth and embryonic epidermal morphogenesis. *PLoS Genet* 5(10):e1000675.
32. Harterink M, et al. (2011) A SNX3-dependent retromer pathway mediates retrograde transport of the Wnt sorting receptor Wntless and is required for Wnt secretion. *Nat Cell Biol* 13(8):914–923.
33. Treusch S, et al. (2004) *Caenorhabditis elegans* functional orthologue of human protein h-mucolipin-1 is required for lysosome biogenesis. *Proc Natl Acad Sci USA* 101(13):4483–4488.
34. Itoh T, et al. (2005) Dynamin and the actin cytoskeleton cooperatively regulate plasma membrane invagination by BAR and F-BAR proteins. *Dev Cell* 9(6):791–804.
35. Ho HY, et al. (2004) Toca-1 mediates Cdc42-dependent actin nucleation by activating the N-WASP-WIP complex. *Cell* 118(2):203–216.
36. Welchman DP, Mathies LD, Ahringer J (2007) Similar requirements for CDC-42 and the PAR-3/PAR-6/PKC-3 complex in diverse cell types. *Dev Biol* 305(1):347–357.
37. Xin X, et al. (2013) SH3 interactome conserves general function over specific form. *Mol Syst Biol* 9:652.
38. Ang AL, Fölsch H, Koivisto UM, Pypaert M, Mellman I (2003) The Rab8 GTPase selectively regulates AP-1B-dependent basolateral transport in polarized Madin-Darby canine kidney cells. *J Cell Biol* 163(2):339–350.
39. Kroschewski R, Hall A, Mellman I (1999) Cdc42 controls secretory and endocytic transport to the basolateral plasma membrane of MDCK cells. *Nat Cell Biol* 1(1):8–13.
40. Reaves B, Horn M, Banting G (1993) TGN38/41 recycles between the cell surface and the TGN: Brefeldin A affects its rate of return to the TGN. *Mol Biol Cell* 4(1):93–105.
41. Humphrey JS, Peters PJ, Yuan LC, Bonifacino JS (1993) Localization of TGN38 to the trans-Golgi network: Involvement of a cytoplasmic tyrosine-containing sequence. *J Cell Biol* 120(5):1123–1135.
42. Ponnambalam S, et al. (1996) Primate homologues of rat TGN38: Primary structure, expression and functional implications. *J Cell Sci* 109(Pt 3):675–685.
43. Ghosh RN, Mallet WG, Soe TT, McGraw TE, Maxfield FR (1998) An endocytosed TGN38 chimeric protein is delivered to the TGN after trafficking through the endocytic recycling compartment in CHO cells. *J Cell Biol* 142(4):923–936.
44. Maxfield FR, McGraw TE (2004) Endocytic recycling. *Nat Rev Mol Cell Biol* 5(2):121–132.
45. Ponnambalam S, Rabouille C, Luzio JP, Nilsson T, Warren G (1994) The TGN38 glycoprotein contains two non-overlapping signals that mediate localization to the trans-Golgi network. *J Cell Biol* 125(2):253–268.
46. Wong SH, Hong W (1993) The SXYQRL sequence in the cytoplasmic domain of TGN38 plays a major role in trans-Golgi network localization. *J Biol Chem* 268(30):22853–22862.
47. Prasad BC, Clark SG (2006) Wnt signaling establishes anteroposterior neuronal polarity and requires retromer in *C. elegans*. *Development* 133(9):1757–1766.
48. Coudreuse DY, Roël G, Betist MC, Destrée O, Korswagen HC (2006) Wnt gradient formation requires retromer function in Wnt-producing cells. *Science* 312(5775):921–924.
49. Wassmer T, et al. (2009) The retromer coat complex coordinates endosomal sorting and dynein-mediated transport, with carrier recognition by the trans-Golgi network. *Dev Cell* 17(1):110–122.
50. Lorenowicz MJ, et al. (2014) Inhibition of late endosomal maturation restores Wnt secretion in *Caenorhabditis elegans* vps-29 retromer mutants. *Cell Signal* 26(1):19–31.
51. Pan CL, et al. (2006) Multiple Wnts and Frizzled receptors regulate anteriorly directed cell and growth cone migrations in *Caenorhabditis elegans*. *Dev Cell* 10(3):367–377.
52. Seaman MN, Gautreau A, Billadeau DD (2013) Retromer-mediated endosomal protein sorting: All WASHed up! *Trends Cell Biol* 23(11):522–528.
53. Pfeffer SR (2011) Entry at the trans-face of the Golgi. *Cold Spring Harb Perspect Biol* 3(3):a005272.
54. Lin SX, Mallet WG, Huang AY, Maxfield FR (2004) Endocytosed cation-independent mannose 6-phosphate receptor traffics via the endocytic recycling compartment en route to the trans-Golgi network and a subpopulation of late endosomes. *Mol Biol Cell* 15(2):721–733.
55. Hutagalung AH, Novick PJ (2011) Role of Rab GTPases in membrane traffic and cell physiology. *Physiol Rev* 91(1):119–149.
56. Ang SF, Fölsch H (2012) The role of secretory and endocytic pathways in the maintenance of cell polarity. *Essays Biochem* 53:29–39.
57. Pocha SM, Wassmer T, Niehage C, Hoflack B, Knust E (2011) Retromer controls epithelial cell polarity by trafficking the apical determinant Crumbs. *Curr Biol* 21(13):1111–1117.
58. Zhou B, Wu Y, Lin X (2011) Retromer regulates apical-basal polarity through recycling Crumbs. *Dev Biol* 360(1):87–95.
59. Estravís M, Rincón SA, Santos B, Pérez P (2011) Cdc42 regulates multiple membrane traffic events in fission yeast. *Traffic* 12(12):1744–1758.
60. Steenblock C, et al. (2014) The Cdc42 guanine nucleotide exchange factor FGD6 coordinates cell polarity and endosomal membrane recycling in osteoclasts. *J Biol Chem* 289(26):18347–18359.
61. Hu J, et al. (2009) F-BAR-containing adaptor CIP4 localizes to early endosomes and regulates Epidermal Growth Factor Receptor trafficking and downregulation. *Cell Signal* 21(11):1686–1697.
62. Patel FB, Soto MC (2013) WAVE/SCAR promotes endocytosis and early endosome morphology in polarized *C. elegans* epithelia. *Dev Biol* 377(2):319–332.
63. Frost A, et al. (2008) Structural basis of membrane invagination by F-BAR domains. *Cell* 132(5):807–817.
64. Suetsugu S, Toyooka K, Senju Y (2010) Subcellular membrane curvature mediated by the BAR domain superfamily proteins. *Semin Cell Dev Biol* 21(4):340–349.
65. Itoh T, De Camilli P (2006) BAR, F-BAR (EFC) and ENTH/ANTH domains in the regulation of membrane-cytosol interfaces and membrane curvature. *Biochim Biophys Acta* 1761(8):897–912.
66. Suetsugu S (2013) Activation of nucleation promoting factors for directional actin filament elongation: Allosteric regulation and multimerization on the membrane. *Semin Cell Dev Biol* 24(4):267–271.
67. Bisi S, et al. (2013) Membrane and actin dynamics interplay at lamellipodia leading edge. *Curr Opin Cell Biol* 25(5):565–573.
68. Chen B, et al. (2014) The WAVE regulatory complex links diverse receptors to the actin cytoskeleton. *Cell* 156(1-2):195–207.
69. Kaksonen M, Toret CP, Drubin DG (2006) Harnessing actin dynamics for clathrin-mediated endocytosis. *Nat Rev Mol Cell Biol* 7(6):404–414.
70. Römer W, et al. (2010) Actin dynamics drive membrane reorganization and scission in clathrin-independent endocytosis. *Cell* 140(4):540–553.
71. Roux A, Uyhazi K, Frost A, De Camilli P (2006) GTP-dependent twisting of dynamin implicates constriction and tension in membrane fission. *Nature* 441(7092):528–531.
72. Temkin P, et al. (2011) SNX27 mediates retromer tubule entry and endosome-to-plasma membrane trafficking of signalling receptors. *Nat Cell Biol* 13(6):715–721.
73. Puthenveedu MA, et al. (2010) Sequence-dependent sorting of recycling proteins by actin-stabilized endosomal microdomains. *Cell* 143(5):761–773.
74. Timmons L, Fire A (1998) Specific interference by ingested dsRNA. *Nature* 395(6705):854.
75. Kamath RS, et al. (2003) Systematic functional analysis of the *Caenorhabditis elegans* genome using RNAi. *Nature* 421(6920):231–237.
76. Praitis V, Casey E, Collar D, Austin J (2001) Creation of low-copy integrated transgenic lines in *Caenorhabditis elegans*. *Genetics* 157(3):1217–1226.
77. Schweinsberg PJ, Grant BD (2013) *C. elegans* gene transformation by microparticle bombardment. *WormBook* 1–10.
78. Sato M, et al. (2005) *Caenorhabditis elegans* RME-6 is a novel regulator of RAB-5 at the clathrin-coated pit. *Nat Cell Biol* 7(6):559–569.
79. Clokey GV, Jacobson LA (1986) The autofluorescent "lipofuscin granules" in the intestinal cells of *Caenorhabditis elegans* are secondary lysosomes. *Mech Ageing Dev* 35(1):79–94.
80. Hermann GJ, et al. (2005) Genetic analysis of lysosomal trafficking in *Caenorhabditis elegans*. *Mol Biol Cell* 16(7):3273–3288.
81. Grant B, et al. (2001) Evidence that RME-1, a conserved *C. elegans* EH-domain protein, functions in endocytic recycling. *Nat Cell Biol* 3(6):573–579.